Flight and Wind-Tunnel Investigations on Boundary-Layer Transition

K. H. Horstmann,* A. Quast,* and G. Redeker†
Deutsche Forschungsanstalt für Luft- und Raumfahrt (DLR), Braunschweig, Federal Republic of Germany

Flight and wind-tunnel experiments have been carried out to measure the pressure distribution and the transition location on a special wing glove. By means of the linear stability theory of laminar boundary layers limiting N values of Tollmien-Schlichting waves at the transition location have been evaluated. The values of $N \approx 13.5$ are nearly independent of Reynolds number and are the same in flight and wind-tunnel tests.

Nomenclature

A = amplitude of amplified Tollmien-Schlichting waves in the laminar boundary layer
A_0 = initial amplitude of waves in the laminar boundary layer at the instability point
c_p = static pressure coefficient on wing contour
f = frequency of Tollmien-Schlichting waves, s^{-1}
l = chord length of reference wing section, m
N = amplification exponent or N factor after linear stability theory obtained after integration of local amplification rates, $= \ln(A/A_0)$
Re = Reynolds number based on reference chord
Re_T = Reynolds number based on length of laminar boundary layer
x = streamwise coordinate of wing section, m
x/l = dimensionless coordinate in streamwise direction

Introduction

THE crucial point in the design process of laminar airfoils is the prediction of the transition location. It is only possible to estimate the performance of such airfoils, e.g., the drag polars with the laminar drag bucket, with confidence, if reliable transition criteria can be used. Although the development of computational fluid dynamics reached a high standard and high-speed computers are available, the pure calculation of the transition process and especially the transition location is not yet possible.

All transition prediction methods are more or less empirical and need some experimental input. It is obvious that various transition criteria show a broad scatterband depending on the kind and the quality of the data from which they have been derived, e.g., experiments from different wind tunnels or data from flight tests. On the other hand, transition criteria can only be applied reasonably in that data region which has formed the basis of the criterion.

The well-known empirical criteria of Granville[1] and Michel[2] are based on wind-tunnel data taken at low Reynolds numbers and therefore cannot be used for an airfoil design for higher Reynolds numbers in the region of $Re = 10 \times 10^6$. For this reason, it was decided to carry out transition investigations with the following objectives: perform transition investigations on a suitable wing in flight and in wind tunnel by carefully planned and executed measurements. From these experiments, a reliable transition-prediction procedure and a reasonable correlation procedure between flight and wind-tunnel data should be evaluated.

Transition Prediction with the N-Factor Method

A more reliable and sophisticated procedure to detemine the transition location compared to simple empirical laws is the application of the e^N- or N-factor method.[3-6] Based on the stability theory of laminar boundary layers,[7] this method allows the calculation of amplification rates of disturbances of various wavelengths and frequencies, the so-called Tollmien-Schlichting (TS) waves (Fig. 1). From these amplification rates, the amplification ratio and the amplification exponent N can be determined. If it is assumed that a disturbance has a basic amplitude A_0 when it starts amplifying, then the amplification ratio A/A_0 at any point can be calculated by integrating the amplification rates up to this point. The amplification ratio can be expressed by an exponential function e^N where N is the amplification exponent or the so-called N factor. It describes the growth of disturbances and must be evaluated for various wavelengths and frequencies so that N becomes a maximum value.

The use of the linear stability theory for transition prediction for engineering purposes can be described as follows: From carefully performed experiments, the maximum calculated N factor at the experimentally determined transition location will be evaluated and will serve as a limiting N value in a transition-prediction process.[8] The transition location is assumed to be that chordwise position where increased wall shear stress occurs, made visible by the infrared image technique or other methods. For this reason adequate experiments

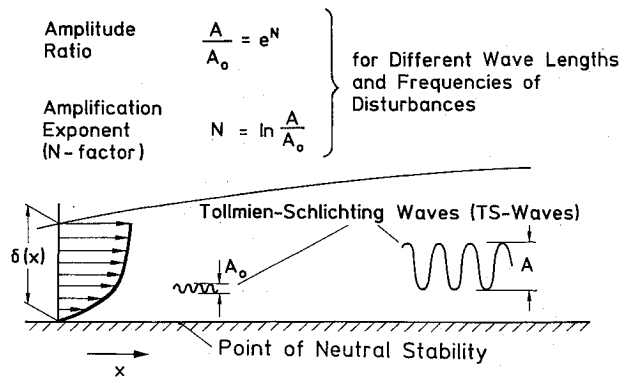

Fig. 1 Instability of laminar boundary layers.

Presented as Paper 88-3.7.1 at the 16th Congress of the International Council of the Aeronautical Sciences, Jerusalem, Israel, Aug. 28-Sept. 2, 1988; received Dec. 21, 1988; revision received July 24, 1989.

*Research Engineer, Institute for Design Aerodynamics.
†Head, Section Airframe Aerodynamics, Institute for Design Aerodynamics.

should include the pressure distribution, and the transition location on wing surface for the same flow conditions. The first item is needed to perform a boundary-layer calculation followed by a stability analysis with N-factor integration, whereas the second item is necessary for the determination of the limiting N value.

Test Aircraft

Flight and wind tunnel tests were carried out with the aircraft shown in Fig. 2. This is a four-seat, experimental prototype light aircraft. Its airframe is built completely out of glass-fiber reinforced plastic. It is a prototype and made its first flight in 1968 with the main objective of studying the effect of weight reduction by the use of lightweight plastics.

The main dimensions are given in Fig. 2. The maximum cruising speed is 330 km/h leading to a Reynolds number of $Re \approx 10 \times 10^6$ based on the aerodynamic mean chord. The small negative leading-edge sweep angle of -4 deg does not have any consequences on the planned investigations. The wing is equipped with an Eppler-airfoil E502, which is not well suited to the purpose of the investigations, as shown in Fig. 3. The pressure distribution on the upper surface, calculated with the Eppler-Somers code,[9] is of such type that transition possibly will take place through a small laminar separation bubble. This is confirmed by a stability analysis with the SALLY code,[10] shown below the pressure distribution. For different frequencies of TS waves, the N-factor development along the airfoil chord is plotted. It leads to an exponential rise in the region of the slight adverse pressure gradient. This behavior at low N factors indicates the existence of a laminar separation bubble, and it is not suited for the determination of limiting N values, as described before. When trying to cut the N-factor curves with steep gradients at the measured transition location, with the line $x/l = \text{const}$, small changes in Δx will result in large changes of the limiting N values (cf. Ref. 6).

A new wing section similar to the E502 airfoil has been designed to overcome the described difficulties. Figure 4 shows the pressure distribution of the new design for the same flight conditions as before. The upper surface of the new design shows a slight pressure rise from 20 to 70% of the airfoil chord leading to an unstable laminar boundary layer, which should run into transition before laminar separation will occur in the rear part of the airfoil. The development of the N factors for TS waves of various frequencies shows the desired behavior: a nearly linear rise with increasing chord length. With this type of behavior it is easy to determine limiting N values at the transition location because a clear cut between the N-factor curve and $x/l = \text{const}$ can be made.

Figure 5 shows a comparison of the new wing section wrapped around the original. The main differences occur on the upper surface near the airfoil leading edge and in the region from 50 to 70% of airfoil chord; the contour of the lower surface remains nearly unchanged. There is a minimum space of 5 mm between the new contour and the original one allowing the installation of the tubing for the pressure orifices. There are 74 pressure orifices of 0.3 mm diam distributed around the airfoil contour with a very dense distribution in the estimated transition region on the upper surface.

A glove on the right wing with this new wing section has been constructed as shown in Fig. 2. It is also made from glass-fiber reinforced plastic and contains the pressure tubing. The inner spanwise location of the glove is defined by the propeller slipstream and at the outer part by the beginning of the aileron. The pressure orifices are arranged on an oblique line compared to the streamwise direction in order to avoid disturbances from orifices lying in a line.

The transition location is determined by means of the infrared technique, which is described in detail in Ref. 11. The infrared camera is installed inside the cabin of the aircraft as shown in Fig. 2 looking at the upper surface of the glove. The

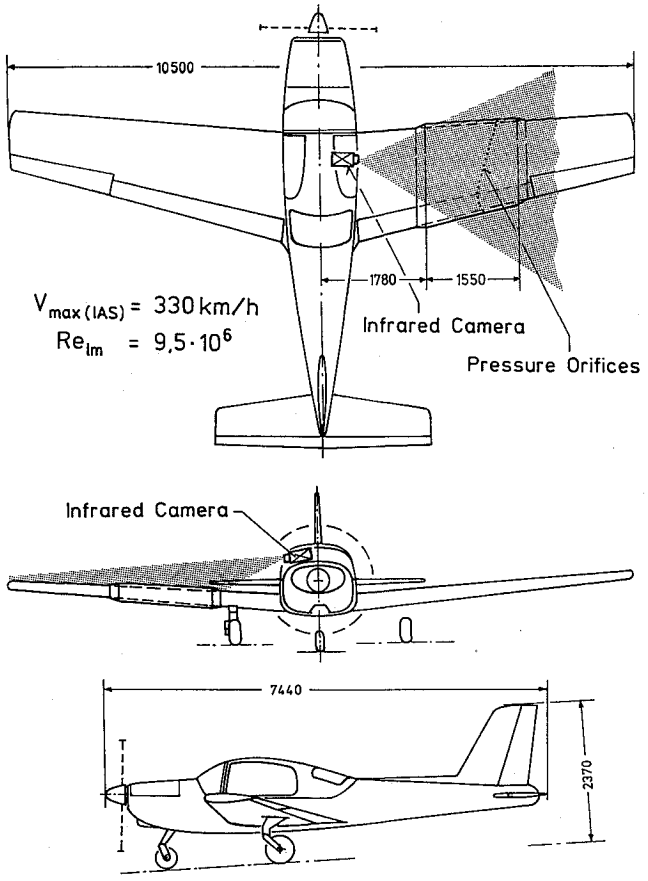

Fig. 2 Installation of the glove and the infrared camera on the test aircraft.

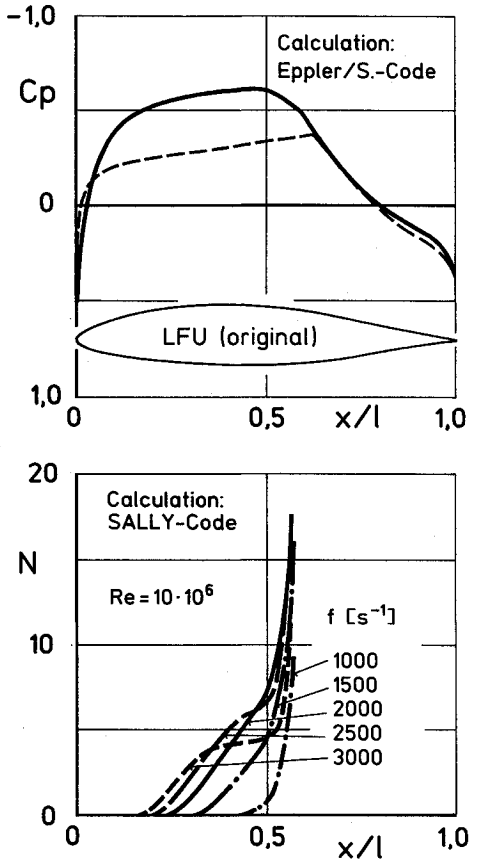

Fig. 3 Pressure distribution and growth of N factor of TS waves on the original wing.

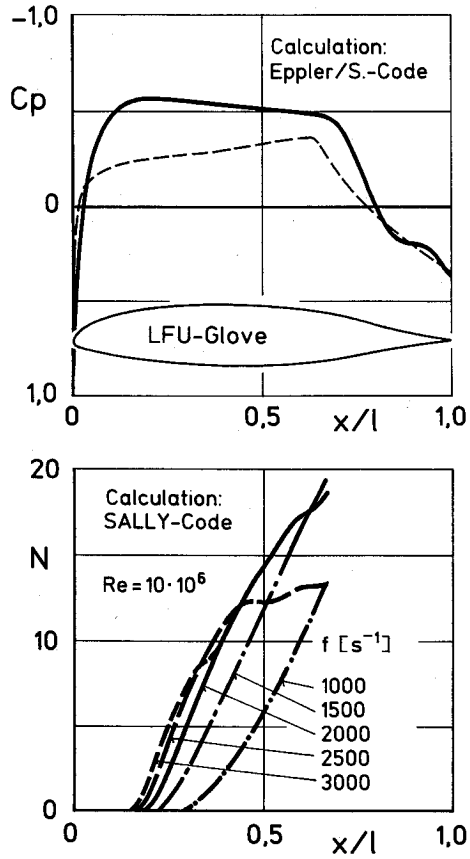

Fig. 4 Pressure distribution and growth of N factor of TS waves on the glove.

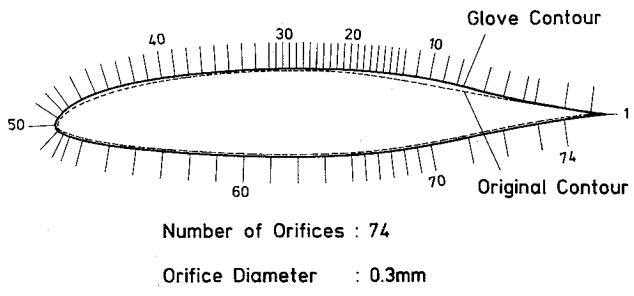

Fig. 5 Comparison of original and glove contour.

advantage of this transition-detection technique is the ability to inspect the complete glove surface. Thus, the transition data for the whole area are available and not just at one point, as provided by some other methods (e.g., hot films).

Flight and pressure data are acquired by a flight measurement system based on a small computer. The pressure data can be inspected in flight by a quick-look system. All data are stored on a data cassette and will be evaluated on ground.

Flight Tests

Aerodynamic flight tests were carried out with different flap deflections, in a speed range from 150–330 km/h, at flight levels between 4000 and 10,000 ft resulting in chord length Reynolds numbers of 3–10 million. Significant changes in flight mechanics due to the glove were not observed. In order to avoid turbulence by thermal convection, all measurements took place in flight levels above a temperature inversion. A typical flight test result will be demonstrated in the next figures.

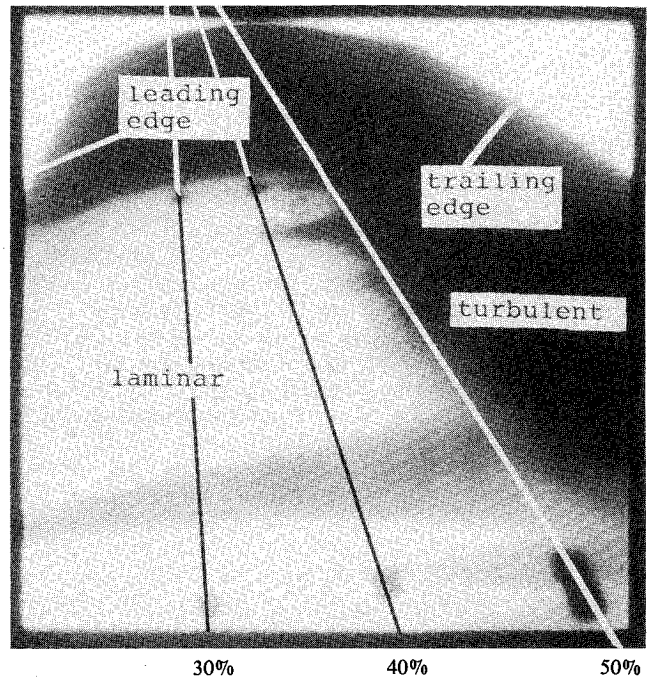

Fig. 6 Infrared image of the glove in flight.

An infrared image of the upper side of the glove at $Re = 9.5 \times 10^6$ is shown in Fig. 6. The bright color in the front part of the glove indicates the laminar boundary layer, whereas the dark color at the rear part of the wing represents the turbulent boundary layer. Transition occurs at 47% of the chord length and can easily be detected by the distinct change in color. The turbulent wedge in the foreground is induced by an artificial roughness.

The corresponding upper side pressure distribution is shown in the upper part of Fig. 7, marked by the circles. It is the typical design pressure distribution of the glove described in Chap. 3. The transition location, found by means of the infrared system, is indicated by an arrow.

The results of the boundary-layer stability analysis of the measured pressure distribution by means of the SALLY code are given in the lower part of Fig. 7. Amplification factors N selected out of all frequencies investigated are shown vs the chordwise position. At the transition location, the envelope leads to a limiting N value of $N \approx 13.5$.

Wind-Tunnel Tests

Although flight tests are very close to reality, experiments in the German-Dutch wind tunnel (DNW) with the real aircraft wing have been carried out. Wind-tunnel tests are often cheaper than flight tests and certain experiments can only be done there. The main objective of the wind-tunnel tests was the determination of a correlation between transition in free flight and DNW, thus qualifying DNW for laminar-flow investigations. It should be noted here that the DNW transition data cannot be transfered to other wind tunnels, due to differences in flow quality. The right wing was installed in the 6×8-m^2 closed test section as shown in Fig. 8. The wing was erected vertically in the test section on a steel spike that fits into the wing spar. Because of restrictions on wing strength only parts of the glove section polars could be measured (e.g., maximum lift at maximum speed will overstress the wing). The same measurements were carried out as in flight.

Figure 9 gives the pressure distribution, transition location, and calculated N factors for the high-speed case at the maximum Reynolds number of $Re = 9.5 \times 10^6$. Transition, detected by an infrared image, takes place at $x/l = 0.40$ and is marked by an arrow.

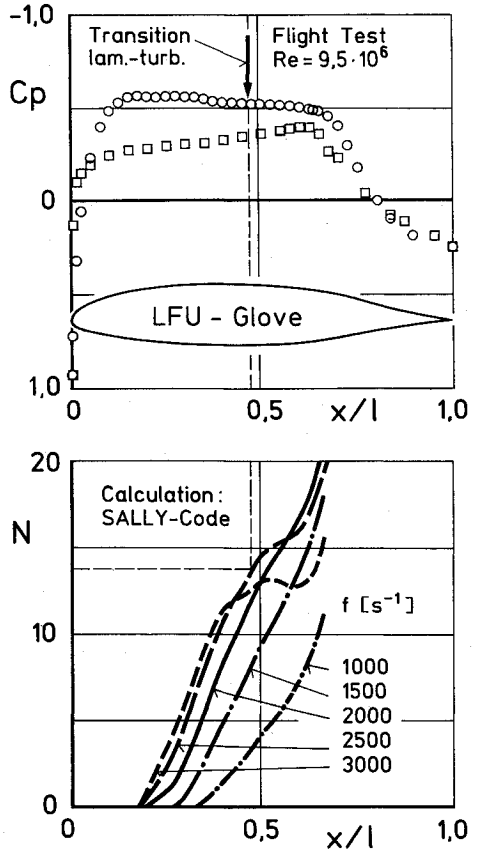

Fig. 7 Flight test pressure distribution and growth of N factor of the TS waves on the glove.

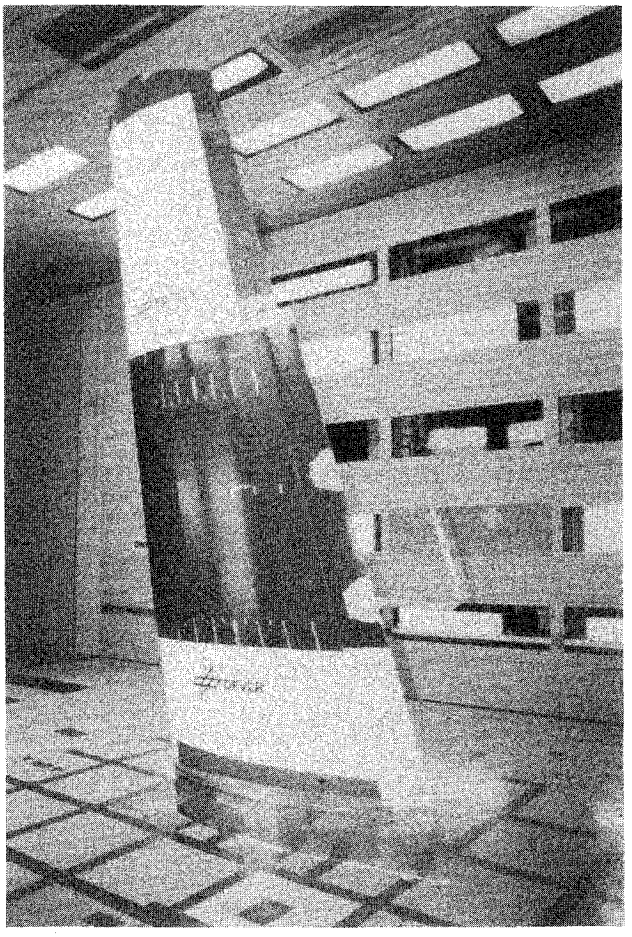

Fig. 8 Wing in the $6 \times 8\text{-m}^2$ test section of DNW.

The stability analysis of the measured pressure distribution is shown by the N-factor development at selected frequencies along the wing chord. At the transition location $x/l = 0.4$, a maximum value of $N \approx 13$ is achieved in a frequency range of $f \approx 3000$ Hz. Higher values of f, not shown here, will result in lower N factors. Thus the limiting N value is $N = 13$.

The comparison of the pressure distributions measured in the DNW (Fig. 9) and in free flight (Fig. 7) shows that although the same flow conditions existed, some remarkable differences are evident. In the wind tunnel the transition location is shifted forward to $x/l = 0.40$ and the pressure distribution shows a small depression in that region. This is due to different deformation of the wing in the wind tunnel and in flight caused by a higher dynamic pressure in the wind tunnel at the same Reynolds number (temperature effect) and by the different wing mounting in wind tunnel and free flight. This effect does not have any consequences on the data evaluation, because differences in pressure distribution will be considered in the stability analysis of the corresponding laminar boundary layer.

The preceding procedure has been applied to several data points with various pressure distributions obtained at different angles of attack, Reynolds numbers, and flap settings.

Figure 10 shows the corresponding infrared image of the wing glove. The flow is from left to right and the laminar boundary layer is indicated by the dark region, whereas the turbulent boundary layer is the white region. A transition line is clearly visible at 40% of the wing chord. The effect of the pressure holes on the transition location in the upper part of the photograph can be detected where a small forward shift of the transition line is visible. For the determination of the N factors, the undisturbed transition location has been used.

Correlation Between Flight and Wind-Tunnel Tests

In Fig. 11, the limiting N values have been collected and are plotted against the Reynolds number Re_T based on the length

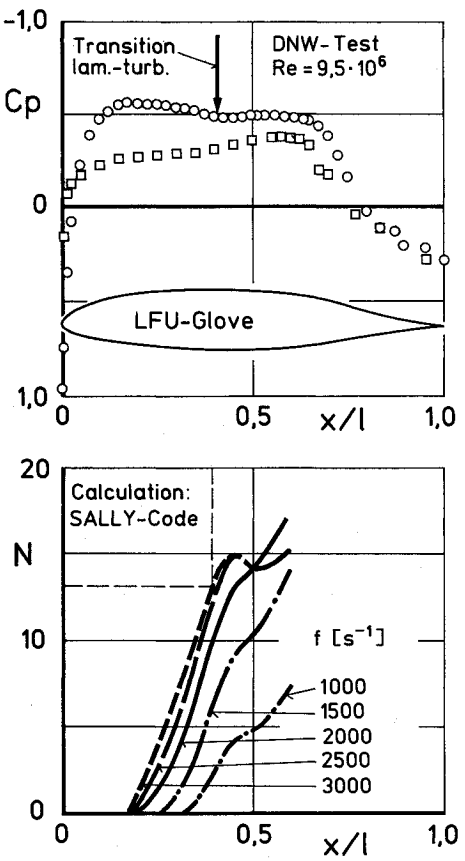

Fig. 9 DNW test pressure distribution and growth of N factor of TS waves on the glove.

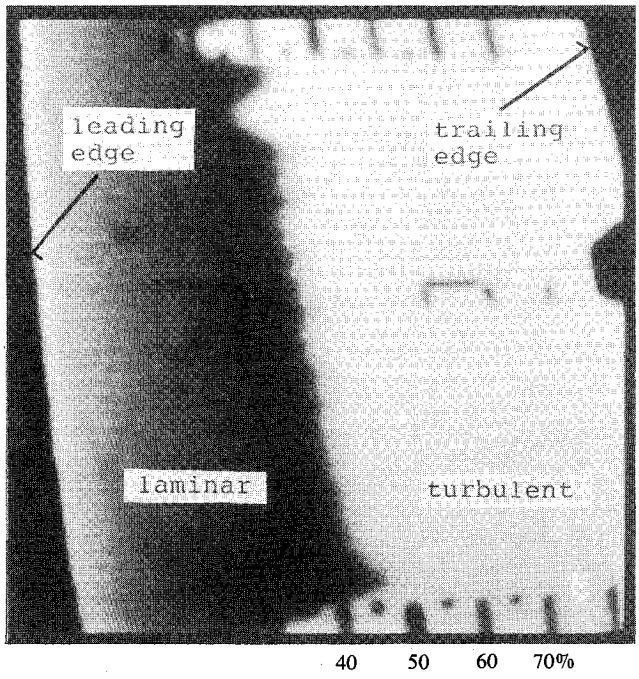

Fig. 10 Infrared image of the glove in DNW.

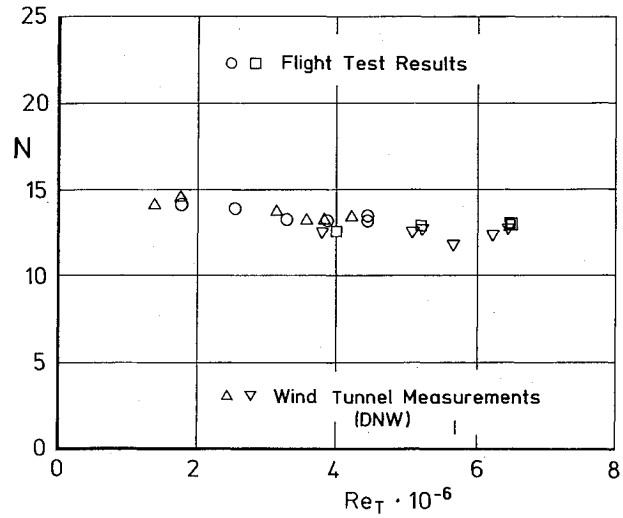

Fig. 11 Calculated N factors of TS waves at transition based on flight and wind-tunnel tests (○ △: 0 deg flap; □ ▽: 3.5 deg flap).

of the laminar boundary layer. The Re_T varies from 1×10^6 to 7×10^6. Each data point has a different pressure distribution, which at the lowest Reynolds number shows a distribution with an adverse pressure gradient at high-lift coefficient, whereas at the highest Reynolds number pressure distributions with zero pressure gradient have been investigated.

Two sets of data are indicated in Fig. 11, and each set of data contains points at two different flap settings. Two remarkable points should be noted here. The limiting N values are nearly independent of the Reynolds number and of the pressure distribution, although a slight decrease with Reynolds number can be seen. The limiting N values of TS waves are $N \approx 13.5$. There is only a small difference between wind tunnel and flight tests in the limiting N values.

The values of $N \approx 13.5$ are rather low values for free-flight tests. It is possible that the presence of engine and propeller noise and structural vibrations may influence the transition behavior. First flight tests, however, showed that the propeller rpm seems to have no visible effect on transition. Further flight tests with engine off, to be performed in the near future, will help clarify the situation.

The values of $N \approx 13.5$ for the DNW data indicate the excellent flow quality of this wind-tunnel test section. A stability analysis of earlier measurements in a low turbulence wind tunnel[12] gave limiting N values of $N \approx 12$. But one has to bear in mind that for these experiments a different method for the transition location detection had been used.

With the knowledge of the relationship between N values from flight and DNW tests, a good correlation concerning the transition behavior is established.

Conclusions

Flight and wind-tunnel investigations concerning boundary-layer transition have been performed with a four-seat aircraft. With carefully planned and executed experiments and a subsequent stability analysis of the laminar boundary layer, limiting N values of Tollmien-Schlichting waves in free flight and in the $6 \times 8\text{-m}^2$ test section of DNW have been evaluated. These values will serve as input for transition prediction with the e^N- or N-factor method. The experiments were performed on a wing glove especially designed for this purpose and comprised pressure measurements and transition-location detection by means of infrared images.

From these investigations the following conclusions can be drawn:

1) The N values are nearly independent from the type of pressure distribution and from the transition Reynolds number Re_T in the range $1 \times 10^6 < Re_T < 7 \times 10^6$.

2) Limiting N values of Tollmien-Schlichting waves in free flight of $N \approx 13.5$ have been evaluated.

3) Limiting N values of Tollmien-Schlichting waves in the $6 \times 8\text{-m}^2$ test section of DNW of $N \approx 13.5$ have been evaluated.

4) These N values are in the same order of magnitude as the values for free flight, demonstrating the excellent flow quality of DNW.

5) The detection of the transition location by means of infrared images proved to be simple, reliable, and area covering.

References

[1]Granville, P.S., "The Calculation of the Viscous Drag of Bodies of Revolution," David Taylor Model Basin Rept. 849, 1953.

[2]Michel, R., "Critère de transition et amplification des ondes d'instabilité laminaire," *La Recherche Aéronautique,* Vol. 70, No. 1, 1959, pp. 25-27.

[3]Jaffe, N.A., Okamura, T.T., and Smith, A.M.O., "Determination of Spatial Amplification Factors and Their Application to Predicting Transition," *AIAA Journal,* Vol. 8, Feb. 1970, pp. 301-308.

[4]Runyan, J. and George-Falvy, D., Amplification Factors at Transition on an Unswept Wing in Free Flight and on a Swept Wing in Wind Tunnel," AIAA Paper 79-0267, 1979.

[5]Hefner, J.N. and Bushnell, D.M., "Status of the Linear Boundary-Layer Stability Theory and the e^N Method with Emphasis on Swept-Wing Applications," NASA TP-1645, 1980.

[6]Obara, C. J. and Holmes, B.J., "Flight-Measured Laminar Boundary-Layer Transition Phenomena Including Stability Theory Analysis," NASA TP-2417, 1985.

[7]Schlichting, H., *Boundary-Layer Theory,* 7th ed., McGraw-Hill, New York, 1979, pp. 449-488.

[8]Redeker, G. and Horstmann, K. H., "Die Stabilitätsanalyse als Hilfsmittel beim Entwurf von Laminarprofilen," German Aerospace Research Establishment, Göttingen, FRG, DFVLR-IB, 1986.

[9]Eppler, R. and Somers, D. M., "A Computer Program for the Design and Analysis of Low-Speed Airfoils," NASA TM-80210, 1980.

[10]Skrokowski, A. J. and Orszag, S. A.,"SALLY Level II User's Guide," COSMIC, Athens, Georgia, COSMIC Program LAR-12556, 1979.

[11]Quast, A., "Detection of Transition by Infrared Image Technique," Proceedings of the International Congress on Istrumentation in Aerospace Simulation Facilities, ICIAS '87 Record, 1987, pp. 125-133.

[12]Braslow, A. L. and Visconti, F., "Investigation of Boundary-Layer Reynolds Number for Transition on an NACA 65(215)-114 Airfoil in the Langley Two Dimensional Low-Turbulence Pressure Tunnel," NACA TN-1704, 1948.